https://doi.org/10.5194/egusphere-2022-137
Preprint. Discussion started: 13 May 2022

Environmental Controls on Observed Spatial Variability of Soil Pore Water Geochemistry in Small Headwater Catchments Underlain with Permafrost

Nathan Alec Conroy,[1*] Jeffrey M. Heikoop,[1] Emma Lathrop,[1,2] Dea Musa,[1] Brent D. Newman,[1] Chonggang Xu,[1] Rachael E. McCaully,[3] Carli A. Arendt,[3] Verity G. Salmon,[4] Amy Breen,[5] Vladimir Romanovsky,[6] Katrina E. Bennett,[1] Cathy J. Wilson,[1] and Stan D. Wullschleger[4]

[1]Earth and Environmental Sciences Division, Los Alamos National Laboratory, Bikini Atoll Road, Los Alamos, New Mexico, 87545
[2]Center for Ecosystem Science and Society, Department of Biological Sciences, Northern Arizona University, Flagstaff, AZ, 86011, USA
[3]Department of Marine Earth and Atmospheric Sciences, North Carolina State University, Raleigh, North Carolina, 27695
[4]Biological and Environmental Systems Science Division and Climate Change Science Institute, Oak Ridge National Laboratory, Oak Ridge, Tennessee, 37831
[5]International Arctic Research Center, P.O. Box 757340, University of Alaska, Fairbanks, Alaska 99775-7340 USA
[6]Geophysical Institute, University of Alaska Fairbanks, Fairbanks, Alaska, 99775

Correspondence to: Nathan Alec Conroy (nconroy@lanl.gov)

Abstract. Soil pore water (SPW) chemistry can vary substantially across multiple scales in Arctic permafrost landscapes. The magnitude of these variations and their relationship to scale are critical considerations for understanding current controls on geochemical cycling and for predicting future changes. These aspects are especially important for Arctic change modelling where accurate representation of sub-grid variability may be necessary to predict watershed scale behaviours. Our research goal was to characterize intra- and inter-watershed soil water geochemical variations at two contrasting locations in the Seward Peninsula of Alaska, USA. We then attempt to establish which environmental factors were important for controlling concentrations of important pore water solutes in these systems. The SPW geochemistry of 18 locations spanning two small Arctic catchments were examined for spatial variability and its dominant environmental controls. The primary environmental controls considered were vegetation, soil moisture/redox condition, water/soil interactions and hydrologic transport, and mineral solubility. The sampling locations varied in terms of vegetation type and canopy height, presence or absence of near-surface permafrost, soil moisture, and hillslope position. Vegetation was found to have a significant impact on SPW NO3 concentrations, associated with the localized presence of nitrogen-fixing alders and mineralization and nitrification of leaf litter from tall willow shrubs. The elevated NO3 concentrations were however, frequently equipoised by increased microbial denitrification in regions with sufficient moisture to support it. Vegetation also had an observable impact on soil moisture sensitive constituents, but the effect was less significant. The redox conditions in both catchments were generally limited by Fe reduction, seemingly well-buffered by a cache of amorphous Fe hydroxides, with the most reducing conditions found at sampling locations with the highest soil moisture content. Non-redox-sensitive cations were affected by a wide variety of water-soil interactions that affect mineral solubility and transport. Identification of the dominant controls on current SPW hydrogeochemistry allows for qualitative prediction of future geochemical trends in small Arctic catchments that are likely to experience warming and permafrost thaw. As source

https://doi.org/10.5194/egusphere-2022-137
Preprint. Discussion started: 13 May 2022

areas for geochemical fluxes to the broader Arctic hydrologic system, geochemical processes occurring in these environments are particularly important to understand and predict with regards to such environmental changes.

1. Introduction

Permafrost thaw in the Arctic is causing significant changes to landscape structure (Kokelj and Jorgenson, 2013; Rowland et al., 2010), hydrology (Hiyama et al., 2021; Kurylyk et al., 2021; Liljedahl et al., 2016; Vonk, Tank, and Walvoord, 2019; Walvoord and Kurylyk, 2016), vegetation (Lara, Nitze, Grosse, and McGuire, 2018; Myers-Smith et al., 2011; Sturm, Racine, and Tape, 2001; K. D. Tape, Hallinger, Welker, and Ruess, 2012; K. Tape, Sturm, and Racine, 2006;), and biogeochemistry (O'Donnell et al., 2021; Frey and McClelland, 2009; Salmon et al., 2019; Vonk, Tank, and Walvoord, 2019). The integrated hydrogeochemical effects of these environmental changes are already apparent in the chemistry of the large Arctic rivers, where fluxes of carbon and nutrients are increasing, leading to enhanced nutrient loadings, with strong implications for the global carbon cycle (Bring et al., 2016; Fuchs et al., 2020; McClelland et al., 2016). While the watershed areas of large Arctic rivers are vast, recent studies suggest that solute concentrations in these large rivers are likely controlled by solute generation processes occurring at much smaller scales (Harms and Ludwig, 2016; Koch, Runkel, Striegl, and McKnight, 2013; Shogren et al., 2019; Vonk et al., 2015).

While there is a rapidly growing body of literature focused on observing and understanding environmental changes over time with further Arctic warming, relatively few studies directly address the existing spatial variability, within catchments or across catchments, and we are not aware of any studies that have combined field observations with thermodynamic modelling in an effort to understand the causes of the existing spatial variability. Therefore, we have a limited understanding of the key environmental controls on the spatial distribution of soil pore water solute concentrations. In this study, we quantitatively evaluate the spatial variability of soil pore water (SPW) geochemistry within and between two distinct catchments underlain with permafrost, and then seek to identify the source of the observed spatial variability.

This study takes advantage of a scientifically diverse array of observations and datasets made available by the Next Generation Ecosystem Experiment (NGEE) Arctic project, sponsored by the US Department of Energy Office of Science. Most of the locations studied herein were selected by the NGEE Arctic project to provide co-located measurements in a wide range of vegetation types, nested within representative hillslopes and catchments. Although selected largely to represent a range of vegetation structure, such as shrub abundance and canopy height, these locations also have considerable variability in other environmental parameters including, but not limited to: soil moisture and temperature, presence or absence of near-surface permafrost, and maximum observed thaw depth (**Table 1** and **Table 2**). The vegetation-delineated sampling approach presented here provides an opportunity to not only quantify the biogeochemical variability of SPW in Arctic environments, but also to investigate the root causes of that observed variability. Data from additional sampling locations, available from a collaborative study, were also utilized when possible.

Our overarching hypothesis is that vegetation-type and hillslope position are the dominant controls on spatial variability of SPW geochemistry. Vegetation-type seems likely to have a significant effect on SPW geochemistry both

https://doi.org/10.5194/egusphere-2022-137
Preprint. Discussion started: 13 May 2022

directly and indirectly. Directly, through the increased cycling of some solutes (e.g. increased nitrogen concentrations in the vicinity of alders, which add nitrogen to soils via a symbiotic relationship with nitrogen-fixing bacterium; Salmon et al., 2019), and indirectly, through effects on soil moisture (i.e. evapotranspiration and trapping of snow). Soil moisture will also affect SPW geochemistry, particularly of redox sensitive species, by limiting oxygen diffusion and thus controlling which regions develop anoxic/reducing geochemical conditions. Soil moisture impacts will likely be correlated with vegetation-type as well as hillslope position, and the presence or absence of perching layers, including permafrost, all of which impact the vertical and horizontal drainage characteristics of a watershed. Chemical species that are not redox-sensitive or controlled by biogeochemical reactions are likely to be effected by transport, solubility, and water/sediment/organic matter interactions, and therefore largely controlled by hillslope position as well as soil moisture.

Identifying the dominant controls on solute concentration variability within each catchment and across catchments will facilitate better projections of future soil pore hydrogeochemistry in permafrost landscapes, and how these signatures are related to changing soil moisture and increasing in tundra shrub abundance in a changing Arctic (Bring et al., 2016; Myers-Smith et al., 2011; Prowse, Bring, Mård, and Carmack, 2015; Salmon et al., 2019; Sturm et al., 2001; K. D. Tape et al., 2012; K. Tape et al., 2006; Wrona et al., 2016, 2016). Arctic warming and associated permafrost thaw will increase hydrological connectedness between terrestrial and aquatic environments through deepening of the active layer and the formation of deeper, more coherent groundwater flow paths (Bring et al., 2016; Harms and Jones, 2012; Prowse, Bring, Mård, Carmack, et al., 2015; Prowse, Bring, Mård, and Carmack, 2015). Meanwhile, changes in hydrogeochemical signatures in larger Arctic rivers are likely to originate in smaller catchments (McClelland et al., 2016; Prowse, Bring, Mård, and Carmack, 2015; Shogren et al., 2019; Spence, Kokelj, McCluskie, and Hedstrom, 2015). In this sense, changes in hydrogeochemistry in small Arctic catchments not only impact hydrogeochemistry at much larger scales, but also prognosticate the future hydrogeochemistry of larger Arctic rivers.

2. Methods

2.1 Site Descriptions

This study focuses on two sites with permafrost on the Seward Peninsula of western Alaska, the Teller-27 Catchment and the Kougarok-64 Hillslope (**Figure 1**). The Teller-27 Catchment, henceforth "Teller," is a small (~2.25 km2) headwater catchment located west of mile marker 27 along the Nome-Teller Highway northwest of Nome, Alaska. The Kougarok-64 Hillslope, henceforth "Kougarok," is a hillslope (~2.0 km2) located west of mile marker 64 along the Nome-Taylor Highway northeast of Nome, Alaska. We utilized data from "intensive stations" at both Teller and Kougarok where concentrated, multi-year, co-located observations of soil water chemistry, vegetation characteristics, soil moisture and temperature, and other measurements have been collected as part of the NGEE Arctic Research Project. These are identified as TL# (Teller Station #) or KG# (Kougarok Station #) in **Figure 2** and **Figure 3**, respectively. Teller and Kougarok are not paired watersheds in the classical sense, differing in only one major characteristic, which provides the basis for comparison. Instead, Teller and Kougarok differ in many respects and are

https://doi.org/10.5194/egusphere-2022-137
Preprint. Discussion started: 13 May 2022

both representative of the broad range of hillslope conditions common on the Seward Peninsula. Detailed descriptions of Teller and Kougarok have been published previously (Jafarov et al., 2018; Léger et al., 2019; Philben et al., 2019, 2020; Salmon et al., 2019; Yang et al., 2020), therefore, only the catchment characteristics that are probable sources of variability in SPW chemistry will be highlighted here.

Teller is a discrete catchment with a well-defined central drainage, a vertical declivity of approximately 200 m, and a catchment area of approximately 2.25 km2. Temperature probes, soil pits, coring activities, and geophysical interpretations at Teller have confirmed the catchment is underlain with discontinuous permafrost (Léger et al., 2019). The upper shoulder of Teller (near Station 5, **Figure 2** and **Figure 5**) is underlain with near-surface permafrost and appears to be a degraded peat plateau. The resultant microtopography of the degraded peat and the shallow perching horizon caused by the permafrost creates a landscape of unsaturated peat mounds surrounded by ponds and saturated soils. Downslope of the peat plateau, the Teller hillslope has highly variable soil moisture and vegetation (**Table 1**). The microtopography within the lower footslope looks similar to the upper shoulder, but the peat appears more severely degraded and the cause of the perched water table is less clear. Léger et al. (2019) suggest the presence of permafrost at a depth of 1 – 2 m at Teller Station 9 (**Figure 2**), but the perching could also be caused by a layer of silt, at a depth of approximately 30 cm (Graham et al., 2018). The full extent of permafrost and silt in this region of the catchment remains unknown, but the thaw depth in July 2018 was greater than 1 m and maintained a perched water table (Philben et al., 2020), suggesting perching could be the result of silt rather than permafrost. Vegetation type, moisture content, permafrost extent, and hillslope position for all Teller Stations are summarized in **Table 1**.

Kougarok differs in many ways from Teller, although both have characteristics that are typical of hillslopes on the Seward Peninsula. Kougarok is a convex hillslope, with a vertical declivity of approximately 70 meters. The study area at Kougarok is approximately 2.0 km2. Soil temperature measurements at Kougarok suggest that the vast majority of the site is underlain by shallow continuous permafrost (Romanovsky, Cable, and Dolgikh, 2020a); Kougarok Station 5 is an exception, where the permafrost is deeper (Romanovsky et al., 2020a). The upper shoulder of Kougarok is a well-drained rocky outcrop composed of metagranitic rock (Hopkins et al., 1955; Till, Dumoulin, Werdon, and Bleick, 2011). Saturated soils are not prevalent until the footslope and the lower backslope, where Kougarok Stations 2, 11, 10, 1, and 6 are situated (**Figure 3**). The lower backslope is characterized by persistent saturation between ubiquitous tussocks, formed by the tussock cotton grass Eriophorum vaginatum. The tussock-lichen tundra at Kougarok introduces microtopography and spatially variable saturation; in this sense, the Kougarok tussocks are analogous to the peat mounds and hummocks at Teller, but on different spatial scales and formed by different processes. Kougarok has numerous patches of alder shrubland in an altitudinal band within the upper backslope; it should be emphasized that Teller lacks tussock-lichen tundra and alder (Alnus viridis ssp. fruticosa) shrubs that are a feature of Kougarok. While continuous permafrost largely remains, the Kougarok site appears to be undergoing environmental changes as evidenced by an increase in alder coverage over the past decades (Salmon et al., 2019). Soil profiles underneath the alder patches are rocky with shallow bedrock and warmer permafrost (**Table 2**). Shrub tundra (alder savanna in tussock tundra and willow-birch tundra) dominates the lower backslope, where the annual active layer thickness is typically less than 100 cm. Vegetation type, moisture content, permafrost extent, and hillslope position at all Kougarok stations are summarized in **Table 2**.

https://doi.org/10.5194/egusphere-2022-137
Preprint. Discussion started: 13 May 2022

2.2 Sampling & Analytical Approach

SPWs were sampled using two complimentary techniques. Fiberglass wicks (Frisbee, Phillips, Campbell, and Hendrickx, 2010) were deployed in the upper 30 cm of soils at stations where shallow soils were unsaturated. These wicks were left in place from year-to-year and only replaced if damage was observed or suspected. The sample reservoirs from the wicks were collected whenever possible, usually a few times each summer. MacroRhizons (Rhizosphere Research Products; Netherlands) were used at stations that were more saturated, also targeting the upper 30 cm of soils. Both techniques were used at stations of intermediate saturation, where both could be deployed effectively. MacroRhizons represent a relatively discrete temporal sampling event (minutes to hours), whereas wicks represent a cumulative water collected over longer periods (weeks to months). It is in this sense, that the two techniques are complimentary. Unfortunately, due to saturation variability both techniques could not be used at all stations and conditions at some Kougarok stations were sometimes too dry to collect meaningful volumes of SPW using either method. Additional SPW data from Kougarok were supplemented from a separate study focused on alder-related nutrient dynamics (McCaully et al., In Review.). These data were collected by MacroRhizons and are captured as Kougarok Stations 10 – 13, which were not part of the original stations established by the NGEE Arctic Program. A total of 309 SPW samples from Kougarok were collected and analysed, whereas a total of 89 SPW samples from Teller were collected and analysed.

After collection, SPW cation concentrations were measured in triplicate by inductively coupled plasma optical emission spectroscopy (Optima 2100 DV; PerkinElmer, USA) following US EPA Method 200.7. Inorganic anion concentrations were measured by ion chromatography (DX-600; Dionex, USA) following US EPA Method 300.0. B, F, K, Na, and Si concentrations collected by wicks were excluded from the dataset due to known issues with these ions leeching from fiberglass wick samplers (Perdrial et al., 2014; Wallenberger and Bingham, 2009). This effect is illustrated in Supplementary **Figure 1** and the lack of such an effect for divalent cations is shown in Supplementary **Figure 2**. Comparison of data from wicks and MacroRhizons, along with the observations from (Perdrial et al., 2014), demonstrates that remaining constituents discussed herein were not affected by collection with fiberglass wicks. Alkalinity, pH, and E_H are all critical geochemical parameters that are susceptible to change during storage (Petrone, Hinzman, Shibata, Jones, and Boone, 2007); because of the large amount of data from wicks these parameters were not considered further, except in the context of thermodynamic modelling.

Observations related to vegetation, soil moisture, and permafrost extend were compiled from datasets made available by the NGEE Arctic project and are given for Teller in **Table 1** and for Kougarok in **Table 2**. The reported soil moisture contents were derived from an average of gravimetric measurements (2017 and 2018) and time domain reflectometry measurements (2017 and 2019), and from remotely-sensed P-band Synthetic Aperture Radar (2017). End-of-winter snow depths were measured in March and April of 2016, 2017, and 2018. The annual average ground temperature was measured using in-situ temperature sensors (HOBO U30 DataLogger) at a depth of 1.5 meters below the ground surface (Romanovsky et al., 2020a; Romanovsky, Cable, and Dolgikh, 2020b) and the active layer thicknesses were determined by frost probe in September 2019 at the end of the growing season.

https://doi.org/10.5194/egusphere-2022-137
Preprint. Discussion started: 13 May 2022

2.3 Statistical Analysis

Principal Components Analysis (PCA) and the Mann-Whitney U-Test (MWUT) were both used to investigate dominant environmental controls on solute concentrations in SPWs at Teller and Kougarok. PCA is an exploratory data analysis tool that reduces the dimensionality of large complex datasets and considers how components (i.e. solute concentrations) vary together. Because PCA was predominately used as a screening tool to reveal geochemical correlations that may not have been evident by traditional geochemical causations or inference, a detailed discussion of the PCA results is reserved to the Supplementary Materials. The MWUT was used to test for significant differences in solute concentrations between Teller and Kougarok (inter-site variability) and between stations at each site (intra-site variability). The MWUT is a non-parametric method of challenging a null hypothesis, which in this case is the assumption that the concentrations of a given solute are not systematically greater at either site nor at any particular station. Water chemistry data are typically not normally distributed and thus, non-parametric difference tests such as the MWUT are preferred. The MWUT challenges the distribution of values, not the means. In this work, the level of significance associated with the null hypothesis was operationally defined as 0.05, which equates to a 95 % chance that an observed statistical difference is real and not coincidental. This error rate is operationally defined per contrast (i.e. a 95 % chance that the observed statistical difference in nitrate concentrations between Teller Station 9 and Teller Station 7 is real or that the observed statistical difference in sulphate concentrations between Teller and Kougarok is real) as opposed to familywise (i.e. a 95 % chance that all of the observed/reported statistical differences are real and not coincidental). MWUTs were completed using the methods described in Corder and Foreman (2009) and PCA was completed using packages available in R statistical software, version 3.3.6 (Corder and Foreman, 2009; R Core Team, 2020). For all analyses, concentrations below the method detection limit were operationally defined as half the detection limit, in agreeance with (Helsel, 2005, p. 43). While the emphasis of this study was on site/station (i.e. spatial) variability, it should be recognized that seasonal and inter-annual variability could also be significant. To minimize seasonal forcing on the variability observed, all SPW geochemical data presented were collected during the thaw season between June and September.

2.4 Thermodynamic Modelling

To investigate thermodynamic controls on solute behaviour, particularly solubility limitations, thermodynamic modelling exercises were undertaken using PHREEQC, a thermodynamic geochemical modelling code, and PhreePlot, which facilitates repetitive PHREEQC calculations through looping (Kinniburgh and Cooper, 2011; Parkhurst and Appelo, 2013). Because this study was focused on elucidating the primary geochemical controls on solute concentrations in SPWs and not on developing a rigorous transport model, representative concentrations were used instead of station specific concentrations. Representative “low”, “median”, and “high” concentration conditions were proxied from the 25th, 50th, and 100th concentration percentiles, respectively, taken from both Teller and Kougarok (Supplementary **Table 4**). Meanwhile, representative pH and E_H ranges were determined either through direct measurement (pH), or indirectly by correlating dissolved Fe^{2+} concentrations and pH with a redox condition through geochemical models and the Nernst equation. Modelling exercises were performed at 25 °C utilizing the phreeqc.dat database, with the only modification being the suppression of methane production by inorganic carbonate

https://doi.org/10.5194/egusphere-2022-137
Preprint. Discussion started: 13 May 2022

reduction. Methane production was "turned-off" to maintain carbonate availability under reducing conditions to help identify any possible carbonate minerals that could be precipitating. Because alkalinity was only measured in a small number of samples, carbonate concentration percentiles were estimated from charge imbalances. Alkalinity and charge imbalance were very well correlated in samples where alkalinity was measured (Supplementary **Figure 3**). Although not a particularly rigorous modelling exercise, this approach was sufficient to identify mineral phases that could be controlling solute generation processes through solubility limitations.

3. Results

3.1 Inter-site Variability: Teller versus Kougarok

Mann-Whitney U-Testing revealed that the concentrations of 14 of the 23 constituents analysed were significantly different ($1.96 < |z|$) between Teller and Kougarok (**Table 3**). The effect size, a measure of how significantly different the concentrations were, were large for Na and F; medium-large for K and Si; medium for Al, Oxalate, B, Zn, SO_4, Fe, Ba, Ti, and NO2; and small-medium for Li. The terminology and thresholds for these semi-quantitative differences in correlation were taken from Corder and Foreman (2009). When concentrations were significantly different between the sites, Kougarok generally exhibited the higher concentrations of the two. Only SO_4 concentrations were significantly greater at Teller. The concentrations of Br, NO_3, Sr, PO_4, Mg, Cr, Mn, Cl and Ca were not significantly different between Teller and Kougarok. A summary of the inter-site MWUT results are given in **Table 3** with the constituents that exhibited significant differences between the sites displayed over a darkened background.

3.2 Intra-site Variability: Teller and Kougarok Stations

Mann-Whitney U-Testing was also used to test for intra-site differences between stations at both Teller and Kougarok. Boxplots and compact letter displays are used to visualize the within-site variability of a select group of constituents of interest (COIs), which are given in **Figure 4**. Tables of the results of the intra-site MWUTs for all constituents that were monitored, including those that did not demonstrate some systematic inter-station variability or were not otherwise of interest, are given in the Supplementary Materials.

3.3 Physical Characteristics of Stations (Co-Located Studies)

Controls on the observed spatial variability of SWP solute concentrations at Teller and Kougarok stations were deduced, in part, from differences in physical features and conditions of each station. Quantitative measures of many of these physical characteristics were available from the interdisciplinary studies co-located at the Teller and Kougarok stations. The extent of permafrost, ground temperature, active layer depth, soil moisture content, snow depth, vegetation type, vegetation canopy height, dominant plant functional type, and hillslope position were all complied from these co-located studies. Using these measures, the physical characteristics of each station are summarized in **Table 1** and **Table 2**, grouped by vegetation type.

https://doi.org/10.5194/egusphere-2022-137
Preprint. Discussion started: 13 May 2022

4. Discussion

4.1 Inter-site Variability: Teller versus Kougarok

Mann-Whitney U-testing revealed that SPW concentrations of many constituents were significantly different between Teller and Kougarok (**Table 3**). SPW concentrations of Na, F, K, Si, Al, oxalate, B, Zn, Fe, Ba, Ti, NO2, and Li were all significantly greater at Kougarok than Teller, while only SO_4 concentrations were significantly greater at Teller. Meanwhile, the concentrations of Br, NO_3, Sr, PO_4, Mg, Cr, Mn, Cl, and Ca were not significantly different between the two sites. Overall, the more frequent instance of significantly greater constituent concentrations at Kougarok suggests a systematic cause. The extensive low-gradient toeslope (**Figure 2**) and lack of a well-defined drainage channel at Kougarok, are likely causes of the systematically higher SPW solute concentrations at Kougarok. Water perching, the result of near-surface permafrost in the lower-backslope and toeslope, increases evapotranspiration and, thus, SPW solute concentrations. Meanwhile, the lack of a drainage channel at Kougarok suggests that runoff (and therefore solute exports) is more limited than at Teller. Without a relatively rapid export mechanism such as a stream channel, solute transport is likely limited to interflow within the Kougarok hillslope over much of the thaw season, allowing weathering products to increase to significantly greater concentrations than those observed at Teller, where a well-defined drainage/export mechanism does exist. Field observations from pits at Kougarok confirm the present of interflow at the site. The exception to the general observation of elevated concentrations at Kougarok versus Teller was SO_4. Although the cause of consistently higher SO_4 concentrations at Teller is unclear from the limited scope of this study, it seems likely to be due to a greater abundance of sulfidic bedrock material. The presence of sulfidic bedrock in the vicinity of Teller has been reported by mineral prospecting efforts (Brobst, Pinckney, and Sainsbury, 1971; Herreid, 1966; Mulligan, 1965); we are unaware of any such reports near Kougarok.

4.2 Intra-site Variability: Teller and Kougarok Stations

Our interpretation of the major environmental controls on the observed spatial variability of SPW solute concentrations between stations are shown in **Table 4**. Each of these controls, including vegetation effects, soil moisture and redox effects, weathering, water/soil interactions and hydrological transport effects, and mineral solubility effects, is discussed in detail in the following sections.

4.3 Vegetation Effects

Vegetation can influence hydrogeochemical variability directly via vegetation-induced changes to elemental cycling and soil moisture contents, or indirectly via the secondary impacts changes in soil moisture can have on mineral solubility or on the soil redox condition. The geochemical consequences of solubility and redox conditions are the focus of sections to follow, thus, this section will focus on direct vegetation effects via influences on elemental cycling and soil moisture via evapotranspiration and preferential trapping of snow.

NO_3 was the only COI that showed a distinct effect from vegetation via elemental cycling. Elevated NO_3 concentrations were associated with the presence of alder shrubs and, in some cases, willow shrubs. NO_3 concentrations at both sites were generally low, with the exception of Kougarok Stations 3, 5, and 12, and Teller Station 7 (**Figure 4**). Kougarok Stations 3, 5, and 12 all have a significant alder presence. Alders increase soil nitrogen

https://doi.org/10.5194/egusphere-2022-137
Preprint. Discussion started: 13 May 2022

through a symbiotic relationship with nitrogen-fixing bacteria that reside in their root nodules, thus, an association between NO_3 concentrations and alder vegetation is expected (Salmon et al., 2019).

Perhaps more noteworthy was the elevated NO_3 at Kougarok Station 5 and the lack of elevated NO_3 concentrations at Kougarok Stations 1, 2, 6, 10, and 11. The vegetation type at Kougarok Stations 1, 2, 6, 10, and 11 is alder savanna in tussock tundra, which is a mixed graminoid-shrub tundra with shorter stature and lower density of alder shrubs, yet nonetheless nitrogen input via alder derived nitrogen-fixation is anticipated to occur. The lack of elevated NO_3 suggests either that 1) nitrogen-fixation in alder savanna in tussock tundra is insufficient to result in an increase in NO_3 concentrations, 2) that the Kougarok footslope and lower backslope is very nitrogen-limited, and thus, that NO_3 is largely consumed by vegetation as it is fixed, or 3) that microbes in the Kougarok footslope and lower backslope rapidly denitrify the available NO_3 as a substitute for oxygen in their metabolisms. The smaller shrub size and density in the alder savanna in tussock tundra certainly results in less accumulated leaf litter relative to the denser and larger alder shrubland intensive stations, as such, it seems reasonable that less nitrogen would be available at stations in alder savanna in tussock tundra. Meanwhile, isotopic measurements of nitrogen downslope of alder patches at Kougarok Stations 12 and 3 also support the occurrence of denitrification (McCaully et al., In Review). Therefore, we believe the lack of elevated NO_3 concentrations at Kougarok Stations 1, 2, 6, 10, and 11 is a combination of less alder leaf litter and greater denitrification, than at Kougarok Stations 3, 5, or 12.

At Teller, only Station 7 exhibited elevated NO_3 concentrations relative to the rest of the catchment. Teller Station 7 is dominated by tall willow shrubs and is relatively dry. Mineralization and nitrification of willow leaf litter coupled with limited microbial denitrification is the presumed cause of elevated NO_3 concentrations at Teller Station 7. Teller Station 2 also has tall willow shrubs but did not exhibit elevated NO_3 concentrations. From the limited scope of this study, it is unclear why Teller Station 2 did not exhibit elevated NO_3 while Station 7 did, but we suspect that higher seasonal moisture content and greater microbial denitrification at Teller Station 2 likely played a role. Also of note was that despite significant intra-site NO_3 concentration differences, inter-site differences were not significant ($|z| = 1.59$) and that relatively few Kougarok stations showed elevated NO_3 concentrations, despite a widespread alder presence. Increased microbial denitrification is suspected to balance increased nitrogen-fixation at these stations. This is consistent with previous studies that have noted higher nitrogen mineralization rates in acidic tundra than non-acidic tundra (Weiss et al., 2005); Kougarok is predominantly acidic tundra and Teller is non-acidic tundra.

The effect of vegetation on spatial variability of soil moisture was not readily observed in the volumetric moisture content of soil (**Table 1** and **Table 2**) but was somewhat apparent in the spatial variability of moisture sensitive constituents, such as Cl (**Figure 4**). The lack of a clear correlation between vegetation and soil moisture by TDR or P-band SAR observations is perhaps do to the coarseness of the P-band SAR observations and the strong seasonality associated with both methods. Moisture sensitive constituents, such as Cl, may provide a more seasonally averaged tracer of soil moisture content at the stations. An increase in Cl concentrations with vegetation canopy height was apparent at Teller stations suggesting an evapotranspiration effect. This trend was also apparent at Kougarok, but the differences were rarely significant. Overall, the spatial variability of soil moisture sensitive constituents, like Cl, was far less correlated with vegetation-type than expected; perhaps due to preferential trapping of snow, which may offset

https://doi.org/10.5194/egusphere-2022-137
Preprint. Discussion started: 13 May 2022

the increased evapotranspiration of tall shrubs more than previously realized. Overall, Cl concentrations at Kougarok appeared to be more correlated with hillslope position than with vegetation canopy height (**Figure 4**).

4.4 Soil Moisture and Redox Effects

Soil moisture content can have a profound effect on redox sensitive elements. Saturation limits oxygen diffusion into soil, and thus, forces microorganisms to utilize less energetic electron acceptors to metabolize organic matter. In an ideal system, soil microorganisms will use the strongest electron acceptor available, until it is exhausted. Although natural environments are not ideal systems, redox conditions in soils follow a more or less stepwise progression. Therefore, by evaluating the dissolved concentrations of NO_3, Mn, Fe, and SO_4 in SPWs, it is possible to qualitatively assess soil redox conditions and their impact on hydrogeochemical variability.

The redox conditions at both Teller and Kougarok are generally limited by Fe reduction, with the most reducing conditions found at stations with the highest soil moisture content. As such, NO_3 concentrations are generally low (**Table 3**), SO_4 concentrations are relatively consistent (**Figure 4**), and Mn and Fe concentrations increase with increasing soil moisture (**Figure 4**). NO_3 concentrations were generally low, except for drier stations in the proximity of tall alders or willows. While NO_3 inputs are discussed in the vegetation effects section, the lack of high NO_3 concentrations at wetter stations that contain alders suggests that soil moisture coupled with microbial denitrification bares a strong control on SPW NO_3 concentrations. Meanwhile, SO_4 concentrations at both sites are relatively constant across clear moisture and redox gradients (**Figure 4**). This suggests that SO_4 reduction is not pervasive at either site. Dissolved Fe concentrations were higher at stations with higher soil moisture content, consistent with Fe reduction. Similarly, Mn concentrations were slightly elevated at wetter stations. The concentrations of Mn, however, rarely rose above 0.05 mg·L 1, suggesting either Mn solubility limitations or a lack of a significant Mn weathering source. Low Mn concentrations at Teller Station 5, a wetter station on the upper shoulder of the Teller watershed (**Table 1**; **Figure 2**) seems to support the latter conclusion, as do geochemical modelling exercises (Section 4.5). Together, these results suggest that the most reducing condition at both sites is typically limited to Fe reduction and that this only occurs at stations with the highest soil moisture contents.

4.4 Weathering, Water/Soil Interaction, and Hydrological Transport Effects

A combination of weathering, water/soil interactions, and hydrological transport were clear drivers of hydrogeochemical variability for some solutes. As noted by Philben et al. (2020), soil derived solutes tend to accumulate in low-lying areas within watersheds. This is clearly seen at Teller, where the concentrations of Ca, Sr, and Mg all increase dramatically at the transition from lower backslope to footslope (**Figure 5**). Both Teller and Kougarok are underlain by carbonate-rich metamorphic facies, and Ca, Sr, and Mg are probable carbonate counter-cations. Weathering of Ca, Sr, and Mg carbonates and subsequent transport of these cations downslope explains this pattern of spatial variability. At Kougarok, concentrations of Ca, Mg, and Sr similarly increase from upper backslope to footslope, but concentrations of Ca and Sr decrease further down the lower backslope (Stations 10 and 1), while Mg concentrations continue to increase. A possible explanation for this behaviour is the greater affinity of cation

https://doi.org/10.5194/egusphere-2022-137
Preprint. Discussion started: 13 May 2022

exchange surfaces for Ca and Sr compared to Mg, thus, Ca and Sr are preferentially retained in the footslope whilst Mg is transported further down the lower backslope (Sparks, 2003, p. 189).

4.5 Mineral Solubility Effects

Although redox reactions are rarely at equilibrium in natural environments, comparison of field data with equilibrium models provides valuable semi-quantitative insight into the redox condition of natural environments. Because Fe appeared to be limiting the development of more reducing conditions (Section 4.3), select samples from both sites were measured for soluble Fe^{2+} following methods presented in Viollier et al. (2000). These concentrations of aqueous Fe^{2+} were then compared with model-predicted concentrations of Fe^{2+}, when coupled with an infinite $Fe(OH)_{3(am)}$ phase, across a range of pH values (2 – 10) and fixed E_H values of 400 mV, 200 mV, 0 mV, and -200 mV; activity coefficients were assumed to be equal to 1. The measured and modelled Fe^{2+} concentrations are compared in **Figure 6**, where concentrations that were below the method detection limit (0.05 mg·L-1) are set equal to 0.025 mg·L-1 (half the detection limit). Comparison of model predicted Fe^{2+} concentrations with field data suggests that while Teller exhibits a narrower range of pH conditions than Kougarok, it exhibits a broader range of redox conditions (**Figure 6**). Although several Fe^{2+} measurements were below the detection limit, suggesting oxidizing conditions, high Fe^{2+} concentrations in some samples suggested E_H values below 0 mV. Therefore, Fe redox conditions at Teller ranged from mildly reducing to oxic and Fe redox conditions at Kougarok ranged from mildly oxic to oxic. Oxidation-reduction potentials (ORPs), calculated from pH, Fe^{2+} concentrations, and the Nernst equation suggest that ORPs at Teller were as low as - 69 mV, while the lowest ORP at Kougarok was + 134 mV (**Figure 6**). Maximum ORP values could not be determined quantitatively as some Fe^{2+} concentrations were below Fe^{2+} detection limits, at both sites.

E_H/pH predominance diagrams were created from the 25th, 50th, and 100th concentration percentiles and are shown in **Figure 7** for the COIs where precipitation of mineral phases were predicted under some conditions. The concentrations for these diagrams were taken from filtered aqueous concentration data, thus, predicted mineral precipitation is an indication of nearly saturated or over-saturated conditions. The range of E_H and pH conditions observed at Teller and Kougarok are overlaid as solid yellow and solid blue lines, respectively. Only the predominance diagrams that indicated possible mineral formation under the E_H/pH conditions present at either site are shown in **Figure 7**. These phases included $Fe(OH)_{3(am)}$ (Fe), siderite (Fe), $Al(OH)_{3(am)}$ (Al), chalcedony (Si), barite (Ba and SO_4), calcite (Ca), dolomite (Ca and Mg), and rhodochrosite (Mn). Predominance diagrams for the remaining key COIs that were not predicted to form any mineral phases under any site conditions are given in Supplementary **Figure 4**.

To further examine which mineral phases could be controlling solute generation processes, saturated conditions for the mineral phases identified in **Figure 7** were modelled using sweeps of pH values from 2 – 10 at various fixed E_H values (400mV, 200mV, 0mV, and -200mV). Predicted solute concentrations under the modelled saturated conditions were then compared with field data to find common trends. In general, if solute concentrations were frequently measured near the saturation of a mineral, or were identified to have similar dependence on pH or E_H, it was inferred that the mineral phase could be controlling the generation of that solute. The mineral phases that were identified to possibly be controlling solute concentrations were $Al(OH)_{3(am)}$, $Fe(OH)_{3(am)}$, chalcedony, and barite. This does not

https://doi.org/10.5194/egusphere-2022-137
Preprint. Discussion started: 13 May 2022

preclude the presence of significant concentrations of other mineral phases, it only identifies these as likely controlling the dissolved concentrations of Al, Fe, Si, and Ba, respectively.

Aluminium concentrations in SPWs at both Teller and Kougarok appear to be controlled by the dissolution/precipitation of amorphous Al hydroxide ($Al(OH)_{3(am)}$) (**Figure 8**). The solubility limit of $Al(OH)_{3(am)}$ has no redox dependence, but is highly pH dependent. Aluminium concentrations were generally clustered near the solubility limit of $Al(OH)_{3(am)}$; $Al(OH)_{3(am)} + 3H^+ \leftrightarrow Al^{3+} + 3H_2O$; log k = 10.8. This suggests that Al SPW concentrations at both sites are controlled by wetting/drying (dissolution/precipitation) processes. It also suggests that there could be a significant amount of $Al(OH)_{3(am)}$ in the soils at both sites. While organic matter may also sorb to alumina surfaces, the adherence to the solubility of $Al(OH)_{3(am)}$ suggests that significant concentrations of Al are not complexed with dissolved organic matter. The predominance diagrams highlight 1) the strong pH dependence on the stability of $Al(OH)_{3(am)}$, 2) the influence of dissolved F can have on Al speciation when Al concentrations are low, and 3) that Al is a cation at low pH and an anion at high pH (**Figure 7**). Despite being a weathering product, Al concentrations show a dissimilar downslope trend to other weathering products, especially at Teller (Supplementary **Figure 5**). While the concentrations of weathering products generally increase with distance downslope, Al concentrations decrease. We suspect this can be attributed to increasing pH with distance downslope. Philben et al. (2020) reported a 1 pH unit increase in pH in organic soils along the Teller transect (**Figure 2**), increasing from 5.6 at Station 5 to 6.7 at Station 9. Such an increase would decrease the solubility of $Al(OH)_{3(am)}$, and thus, decrease the concentration of dissolved Al (**Figure 8**).

Similar to Al, Fe concentrations in SPWs at both Teller and Kougarok appear to be controlled by the dissolution/precipitation of amorphous Fe hydroxide ($Fe(OH)_{3(am)}$). Fe concentrations were generally clustered near the solubility limit of $Fe(OH)_{3(am)}$ (**Figure 8**). Unlike $Al(OH)_{3(am)}$ however, $Fe(OH)_{3(am)}$ solubility is dependent on the redox condition in addition to the pH; $Fe(OH)_{3(am)} + 3H^+ + e^- \leftrightarrow Fe^{2+} + 3H_2O$; log k = 16.0 (**Figure 8**). Fe(III) is only sparingly soluble in aqueous solutions and reduction to Fe(II) significantly increases the solubility of Fe, thus, at a given pH value higher aqueous concentrations are predicted and observed under more reducing conditions (**Figure 8**). Iron concentrations in SPWs at both sites generally follow the pH dependence of $Fe(OH)_{3(am)}$ solubility (**Figure 8**). This suggests that SPW concentrations of Fe at both sites are controlled by wetting/drying (dissolution/precipitation) processes, coupled with the redox condition.

Si concentrations are frequently limited by the solubility of chalcedony, a very finely grained form of SiO2, which is much more soluble than quartz; $SiO_2 + 2H_2O \leftrightarrow H_4SiO_4$; log k = - 3.55. Particularly at Kougarok, the dissolved Si concentrations, coupled with a lack of a strong pH or E_H dependence, suggest a controlling influence of chalcedony.

Ba concentrations also appear to be controlled by solubility, but rather than by the solubility of an oxide or a hydroxide phase, by the solubility of barite [$Ba^{2+} + SO_4^{2-} \leftrightarrow BaSO_4(s)$; log k = 9.97]. Unlike Al hydroxide or Fe hydroxide, barite solubility lacks a strong pH dependence and instead is dependent solely on the activities of Ba^{2+} and SO_4^{2-}. Unlike Ba, SO_4 concentrations are not limited by the solubility limit of barite and are generally higher and not well correlated with Ba concentrations. Together, these suggest that SO_4 from another source (likely, atmospheric deposition or sulfidic mineral oxidation), is suppressing barite dissolution, and thus, is reducing dissolved Ba concentrations. Barite solubility can exhibit a redox dependence if conditions are sufficiently reducing to reduce SO_4 to sulphide. This shifts

https://doi.org/10.5194/egusphere-2022-137
Preprint. Discussion started: 13 May 2022

the equilibrium to greater dissolution of barite, and therefore higher conditions of Ba. The lack of E_H dependence in observational data further suggests that neither site exhibits significant SO_4 reduction.

5. Conclusions

5.1 The Dominant Environmental Controls on Spatial Variability of SPW Solute Concentrations

The 18 stations examined herein (8 at Teller and 10 at Kougarok) were selected to represent a wide range of vegetation types, soil moisture contents, permafrost extents, and hillslope positions. Coupling the spatial variability of these landscape characteristics with the spatial variability of SPW solute concentrations provides valuable insight into the dominant environmental controls on observed spatial variability of SPW geochemistry.

With regard to our initial hypotheses, our major findings are that:

Vegetation influences on elemental cycles were only readily apparent for nitrogen and although vegetation induced changes to soil moisture content were discernible, they were far less significant than anticipated. NO_3 was the only COI that exhibited a clear vegetation effect; elevated concentrations were associated with the presence of alder shrubs and, in some cases, tall willow shrubs. These increases in NO_3 concentrations associated with alder nitrogen-fixation and the mineralization and nitrification of willow leaf litter were frequently equipoised by increased microbial denitrification in regions sufficiently moist to support it. Although both Kougarok and Teller exhibited some indications of increased Cl concentrations in the presence of tall shrubs, the net vegetation effect on soil moisture was far less than hypothesized. Redox sensitivity was also less then hypothesized and most stations seemed well-buffered at Fe redox conditions. The result of this buffering was generally low NO_3 concentrations (except where vegetation effects dominated), consistent SO_4 concentrations across clear redox gradients, and variable Mn and Fe concentrations. Mn concentrations were generally low, likely due to a limited source. Fe concentrations were higher at stations with higher soil moisture content, consistent with Fe reduction. Weathering, water/soil interactions, and hydrological transport were clear drivers of variability for Ca, Sr, and Mg. Ca, Sr, and Mg all tended to accumulate in low-lying areas, although Ca and Sr demonstrated greater accumulation potential than Mg, likely via greater affinity of cation exchange surfaces for Ca and Sr compared to Mg. Mineral solubility limitations were the primary controls on Al ($Al(OH)_{3(am)}$), Fe ($Fe(OH)_{3(am)}$), Ba (barite), and Si (chalcedony) concentrations. This suggests that the SPW concentrations of these constituents will remain stable until those mineral phases are exhausted or soil pore hydrochemistry changes sufficiently to alter the solubility of those mineral phases. Changes in redox condition would significantly alter $Fe(OH)_{3(am)}$ solubility, whereas changes in pH conditions would significantly alter $Al(OH)_{3(am)}$ and $Fe(OH)_{3(am)}$ solubility.

Although discerning the environmental controls on spatial variability of SPW solute concentrations provides some high-level insight into the effects changes in landscape character may have on soil pore hydrochemistry, our scope was limited and leveraged on previously available datasets. The significance of SPW in small Arctic headwater catchments as a key initial component in the freshwater hydrologic continuum is under recognized, and such catchments warrant more detailed and systematic investigations.

https://doi.org/10.5194/egusphere-2022-137
Preprint. Discussion started: 13 May 2022

6. Acknowledgements

We would like to thank the Sitnasuak Native Corporation and the Mary's Igloo Native Corporation for their guidance and for allowing us to conduct this research on the traditional homelands of the Inupiat people. Funding was provided by the Next-Generation Ecosystem Experiments (NGEE Arctic) project, supported by the Office of Biological and Environmental Research in the U.S. DOE Office of Science. We wish to thank Lauren Charsley-Groffman and Nathan Wales for their assistance with fieldwork, as well as, George Perkins, Oana Marina, Rose Harris, and Emily Kluk for their assistance with laboratory analyses.

7. Data availability statement

The data that support the findings of this study are made openly available in the NGEE-Arctic data repository at (DOI: 10.5440/1735757).

8. References

Breen, A., Iversen, C., Salmon, V., VanderStel, H., Busey, B., and Wullschleger, S. 2020a:. NGEE Arctic Plant Traits: Plant Community Composition, Kougarok Road Mile Marker 64, Seward Peninsula, Alaska, 2016 [Data set], doi: https://doi.org/10.5440/1465967.

Breen, A., Iversen, C., Salmon, V., VanderStel, H., Busey, B., and Wullschleger, S. 2020b:. NGEE Arctic Plant Traits: Plant Community Composition, Kougarok Road Mile Marker 64, Seward Peninsula, Alaska, 2016 [Data set], doi: https://doi.org/10.5440/1465967.

Bring, A., Fedorova, I., Dibike, Y., Hinzman, L., Mård, J., Mernild, S. H., … Woo, M.-K. 2016: Arctic terrestrial hydrology: A synthesis of processes, regional effects, and research challenges. Journal of Geophysical Research: Biogeosciences, 121: 621–649, doi: https://doi.org/10.1002/2015JG003131.

Brobst, D. A., Pinckney, D. M., and Sainsbury, C. L. 1971: Geology and Geochemistry of the Sinuk River Barite Deposit, Seward Peninsula, Alaska (No. 463 (?)). United States Department of the Interior Geological Survey.

Conroy, N., Heikoop, J., Newman, B., Wilson, C., Arendt, C., Perkins, G., and Wullschleger, S. 2021: Soil Water Chemistry and Water and Nitrogen Isotopes, Teller Road Site and Kougarok Hillslope, Seward Peninsula, Alaska, 2016 - 2019 [Data set], doi: https://doi.org/10.5440/1735757.

Corder, G. W., and Foreman, D. I. 2009: Nonparametric statistics for non-statisticians: a step-by-step approach. Hoboken, N.J:, Wiley, 247 pp.

Frey, K. E., and McClelland, J. W. 2009: Impacts of permafrost degradation on arctic river biogeochemistry. Hydrological Processes, 23: 169–182, doi: https://doi.org/10.1002/hyp.7196.

Frisbee, M. D., Phillips, F. M., Campbell, A. R., and Hendrickx, J. M. H. 2010: Modified passive capillary samplers for collecting samples of snowmelt infiltration for stable isotope analysis in remote, seasonally inaccessible watersheds 1: laboratory evaluation. Hydrological Processes, 24: 825–833, doi: https://doi.org/10.1002/hyp.7523.

https://doi.org/10.5194/egusphere-2022-137
Preprint. Discussion started: 13 May 2022

493 Fuchs, M., Nitze, I., Strauss, J., Günther, F., Wetterich, S., Kizyakov, A., … Grosse, G. 2020: Rapid Fluvio-Thermal
494 Erosion of a Yedoma Permafrost Cliff in the Lena River Delta. Frontiers in Earth Science, 8: 336, doi:
495 https://doi.org/10.3389/feart.2020.00336.
496 Graham, D. E., Kholodov, A., Wilson, C. J., Moon, J.-W., Romanovsky, V. E., and Busey, B. 2018: Soil Physical,
497 Chemical, and Thermal Characterization, Teller Road Site, Seward Peninsula, Alaska, 2016., doi:
498 https://doi.org/10.5440/1342956.
499 Harms, T. K., and Jones, J. B. 2012: Thaw depth determines reaction and transport of inorganic nitrogen in valley
500 bottom permafrost soils. Global Change Biology, 18: 2958–2968, doi: https://doi.org/10.1111/j.1365-
501 2486.2012.02731.x.
502 Harms, T. K., and Ludwig, S. M. 2016: Retention and removal of nitrogen and phosphorus in saturated soils of arctic
503 hillslopes. Biogeochemistry, 127: 291–304, doi: https://doi.org/10.1007/s10533-016-0181-0.
504 Helsel, D. R. 2005: Nondetects and data analysis: statistics for censored environmental data. Hoboken, NJ:, Wiley-
505 Interscience, 250 pp.
506 Herreid, G. 1966: Preliminary geology and geochemistry of the Sinuk River area. Seward Peninsula, Alaska: Alaska
507 Division of Mines and Minerals Geologic Report, 24: 19.
508 Hiyama, T., Yang, D. and Kane, D.L., 2021. Permafrost Hydrology: Linkages and Feedbacks. In Arctic Hydrology,
509 Permafrost and Ecosystems (pp. 471-491). Springer, Cham.
510 Hopkins, D. M., Karlstrom, T. N. V., Black, R. F., Williams, J. R., Pewe, T. L., Fernald, A. T., and Muller, E. H.
511 1955: Permafrost and ground water in Alaska. U.S. Geological Survey Professional Paper 264-F.
512 Jafarov, E. E., Coon, E. T., Harp, D. R., Wilson, C. J., Painter, S. L., Atchley, A. L., and Romanovsky, V. E. 2018:
513 Modelling the role of preferential snow accumulation in through talik development and hillslope groundwater flow in
514 a transitional permafrost landscape. Environmental Research Letters, 13: 105006, doi: https://doi.org/10.1088/1748-
515 9326/aadd30.
516 Kinniburgh, D., and Cooper, D. 2011: PhreePlot: Creating Graphical Output with Phreeqc.
517 Koch, J. C., Runkel, R. L., Striegl, R., and McKnight, D. M. 2013: Hydrologic controls on the transport and cycling
518 of carbon and nitrogen in a boreal catchment underlain by continuous permafrost. Journal of Geophysical Research:
519 Biogeosciences, 118: 698–712, doi: https://doi.org/10.1002/jgrg.20058.
520 Kokelj, S. V., and Jorgenson, M. T. 2013: Advances in Thermokarst Research. Permafrost and Periglacial Processes,
521 24: 108–119, doi: https://doi.org/10.1002/ppp.1779.
522 Kurylyk and Walvoord, 2021 Kurylyk, B.L. and Walvoord, M.A., 2021. Permafrost Hydrogeology. In Arctic
523 Hydrology, Permafrost and Ecosystems (pp. 493-523). Springer, Cham.
524 Lara, M. J., Nitze, I., Grosse, G., and McGuire, A. D. 2018: Tundra landform and vegetation productivity trend maps
525 for the Arctic Coastal Plain of northern Alaska. Scientific Data, 5: 1–10, doi: https://doi.org/10.1038/sdata.2018.58.
526 Léger, E., Dafflon, B., Robert, Y., Ulrich, C., Peterson, J. E., Biraud, S. C., … Hubbard, S. S. 2019: A distributed
527 temperature profiling method for assessing spatial variability in ground temperatures in a discontinuous permafrost
528 region of Alaska. The Cryosphere, 13: 2853–2867, doi: https://doi.org/10.5194/tc-13-2853-2019.

https://doi.org/10.5194/egusphere-2022-137
Preprint. Discussion started: 13 May 2022

Liljedahl, A. K., Boike, J., Daanen, R. P., Fedorov, A. N., Frost, G. V., Grosse, G., … Zona, D. 2016: Pan-Arctic ice-wedge degradation in warming permafrost and its influence on tundra hydrology. Nature Geoscience, 9: 312–318, doi: https://doi.org/10.1038/ngeo2674.

McCaully, R. E., Arendt, C. A., Newman, B. D., Heikoop, J. M., Wilson, C. J., Sevanto, S., … Wullschleger, S. D. In Review.: High Temporal and Spatial Nitrate Variability on an Alaskan Hillslope Dominated by Alder Shrubs. The Cryosphere.

McClelland, J. W., Holmes, R. M., Peterson, B. J., Raymond, P. A., Striegl, R. G., Zhulidov, A. V., … Griffin, C. G. 2016: Particulate organic carbon and nitrogen export from major Arctic rivers. Global Biogeochemical Cycles, 30: 629–643, doi: https://doi.org/10.1002/2015GB005351.

Mulligan, J. J. 1965: Examination of the Sinuk Iron Deposits Seward Peninsula, Alaska. United States Department of the Interior, 37.

Myers-Smith, I. H., Forbes, B. C., Wilmking, M., Hallinger, M., Lantz, T., Blok, D., … Hik, D. S. 2011: Shrub expansion in tundra ecosystems: dynamics, impacts and research priorities. Environmental Research Letters, 6: 045509, doi: https://doi.org/10.1088/1748-9326/6/4/045509.

O'Donnell, J., Douglas, T., Barker, A. and Guo, L., 2021. Changing Biogeochemical Cycles of Organic Carbon, Nitrogen, Phosphorus, and Trace Elements in Arctic Rivers. In Arctic Hydrology, Permafrost and Ecosystems (pp. 315-348). Springer, Cham.

Parkhurst, D., and Appelo, C. A. J. 2013: Description of input and examples for PHREEQC version 3: a computer program for speciation, batch-reaction, one-dimensional transport, and inverse geochemical calculations (USGS Numbered Series No. 6-A43). Reston, VA: U.S. Geological Survey.

Perdrial, J. N., Perdrial, N., Vazquez-Ortega, A., Porter, C., Leedy, J., and Chorover, J. 2014: Experimental Assessment of Passive Capillary Wick Sampler Suitability for Inorganic Soil Solution Constituents. Soil Science Society of America Journal, 78: 486–495, doi: https://doi.org/10.2136/sssaj2013.07.0279.

Petrone, K. C., Hinzman, L. D., Shibata, H., Jones, J. B., and Boone, R. D. 2007: The influence of fire and permafrost on sub-arctic stream chemistry during storms. Hydrological Processes, 21: 423–434, doi: https://doi.org/10.1002/hyp.6247.

Philben, M., Taş, N., Chen, H., Wullschleger, S. D., Kholodov, A., Graham, D. E., and Gu, B. 2020: Influences of hillslope biogeochemistry on anaerobic soil organic matter decomposition in a tundra watershed. Journal of Geophysical Research: Biogeosciences, n/a: e2019JG005512, doi: https://doi.org/10.1029/2019JG005512.

Philben, M., Zheng, J., Bill, M., Heikoop, J. M., Perkins, G., Yang, Z., … Gu, B. 2019: Stimulation of anaerobic organic matter decomposition by subsurface organic N addition in tundra soils. Soil Biology and Biochemistry, 130: 195–204, doi: https://doi.org/10.1016/j.soilbio.2018.12.009.

Prowse, T., Bring, A., Mård, J., and Carmack, E. 2015: Arctic Freshwater Synthesis: Introduction. Journal of Geophysical Research: Biogeosciences, 120: 2121–2131, doi: https://doi.org/10.1002/2015JG003127.

Prowse, T., Bring, A., Mård, J., Carmack, E., Holland, M., Instanes, A., … Wrona, F. J. 2015: Arctic Freshwater Synthesis: Summary of key emerging issues. Journal of Geophysical Research: Biogeosciences, 120: 1887–1893, doi: https://doi.org/10.1002/2015JG003128.

https://doi.org/10.5194/egusphere-2022-137
Preprint. Discussion started: 13 May 2022

R Core Team. 2020: R: A Language and Environment for Statistical Computing. Vienna, Austria:, R Foundation for Statistical Computing. Retrieved from https://www.R-project.org/.

Romanovsky, V., Cable, W., and Dolgikh, K. 2020a:. Soil Temperature and Moisture, Kougarok Road Mile Marker 64, Seward Peninsula, Alaska, beginning 2016 [Data set], doi: https://doi.org/10.5440/1581586.

Romanovsky, V., Cable, W., and Dolgikh, K. 2020b:. Soil Temperature and Moisture, Kougarok Road Mile Marker 64, Seward Peninsula, Alaska, beginning 2016 [Data set], doi: https://doi.org/10.5440/1581586.

Romanovsky, V., Cable, W., and Dolgikh, K. 2020c:. Soil Temperature and Moisture, Teller Road Mile Marker 27, Seward Peninsula, Alaska, beginning 2016 [Data set], doi: https://doi.org/10.5440/1581437.

Romanovsky, V., Cable, W., and Dolgikh, K. 2020d:. Soil Temperature and Moisture, Teller Road Mile Marker 27, Seward Peninsula, Alaska, beginning 2016 [Data set], doi: https://doi.org/10.5440/1581437.

Rowland, J. C., Jones, C. E., Altmann, G., Bryan, R., Crosby, B. T., Hinzman, L. D., … Geernaert, G. L. 2010: Arctic Landscapes in Transition: Responses to Thawing Permafrost. Eos, Transactions American Geophysical Union, 91: 229–230, doi: https://doi.org/10.1029/2010EO260001.

Salmon, V. G., Breen, A. L., Kumar, J., Lara, M. J., Thornton, P. E., Wullschleger, S. D., and Iversen, C. M. 2019: Alder Distribution and Expansion Across a Tundra Hillslope: Implications for Local N Cycling. Frontiers in Plant Science, 10, doi: https://doi.org/10.3389/fpls.2019.01099.

Schuur, E. A. G., McGuire, A. D., Schädel, C., Grosse, G., Harden, J. W., Hayes, D. J., … Vonk, J. E. 2015: Climate change and the permafrost carbon feedback. Nature, 520: 171–179, doi: https://doi.org/10.1038/nature14338.

Shaver, G. R., Billings, W. D., Chapin, F. S., Giblin, A. E., Nadelhoffer, K. J., Oechel, W. C., and Rastetter, E. B. 1992: Global Change and the Carbon Balance of Arctic Ecosystems. BioScience, 42: 433–441, doi: https://doi.org/10.2307/1311862.

Shogren, A. J., Zarnetske, J. P., Abbott, B. W., lannucci, F., Frei, R. J., Griffin, N. A., and Bowden, W. B. 2019: Revealing biogeochemical signatures of Arctic landscapes with river chemistry. Scientific Reports, 9: 1–11, doi: https://doi.org/10.1038/s41598-019-49296-6.

Smith, L. C., Sheng, Y., MacDonald, G. M., and Hinzman, L. D. 2005: Disappearing Arctic Lakes. Science, 308: 1429–1429, doi: https://doi.org/10.1126/science.1108142.

Sparks, D. L. 2003: Environmental soil chemistry (2nd ed). Amsterdam ; Boston:, Academic Press, 352 pp.

Spence, C., Kokelj, S., McCluskie, M., and Hedstrom, N. 2015: Impacts of Hydrological and Biogeochemical Process Synchrony Transcend Scale. In AGU Fall Meeting Abstracts (Vol. 2015).

Sturm, M., Racine, C., and Tape, K. 2001: Increasing shrub abundance in the Arctic. Nature, 411: 546–547, doi: https://doi.org/10.1038/35079180.

Tape, K. D., Hallinger, M., Welker, J. M., and Ruess, R. W. 2012: Landscape Heterogeneity of Shrub Expansion in Arctic Alaska. Ecosystems, 15: 711–724, doi: https://doi.org/10.1007/s10021-012-9540-4.

Tape, K., Sturm, M., and Racine, C. 2006: The evidence for shrub expansion in Northern Alaska and the Pan-Arctic. Global Change Biology, 12: 686–702, doi: https://doi.org/10.1111/j.1365-2486.2006.01128.x.

Till, A. B., Dumoulin, J. A., Werdon, M. B., and Bleick, H. A. 2011: Bedrock geologic map of the Seward Peninsula, Alaska, and accompanying conodont data. US Department of the Interior, US Geological Survey.

https://doi.org/10.5194/egusphere-2022-137
Preprint. Discussion started: 13 May 2022

603 Uren, N. C. 2018: Calcium oxalate in soils, its origins and fate – a review. Soil Research, 56: 443, doi:
604 https://doi.org/10.1071/SR17244.
605 Vonk, J. E., Tank, S. E., Bowden, W. B., Laurion, I., Vincent, W. F., Alekseychik, P., … Wickland, K. P. 2015:
606 Reviews and syntheses: Effects of permafrost thaw on Arctic aquatic ecosystems. Biogeosciences, 12: 7129–7167,
607 doi: https://doi.org/10.5194/bg-12-7129-2015.
608 Vonk, J. E., Tank, S. E., and Walvoord, M. A. 2019: Integrating hydrology and biogeochemistry across frozen
609 landscapes. Nature Communications, 10: 1–4, doi: https://doi.org/10.1038/s41467-019-13361-5.
610 Wallenberger, F. T., and Bingham, P. A. 2009: Fiberglass and Glass Technology: Energy-Friendly Compositions and
611 Applications. Springer Science & Business Media, 479 pp.
612 Walvoord, M. A., and Kurylyk, B. L. 2016: Hydrologic Impacts of Thawing Permafrost—A Review. Vadose Zone
613 Journal, 15, doi: https://doi.org/10.2136/vzj2016.01.0010.
614 Weiss, M., Hobbie, S. E., & Gettel, G. M. (2005). Contrasting Responses of Nitrogen-Fixation in Arctic Lichens to
615 Experimental and Ambient Nitrogen and Phosphorus Availability. Arctic, Antarctic, and Alpine Research, 37(3), 396–
616 401. https://doi.org/10.1657/1523-0430(2005)037[0396:CRONIA]2.0.CO;2
617 Wilson, C., Bolton, R., Busey, R., Lathrop, E., and Dann, J. 2019: End-of-Winter Snow Depth, Temperature, Density
618 and SWE Measurements at Kougarok Road Site, Seward Peninsula, Alaska, 2018 [Data set], doi:
619 https://doi.org/10.5440/1593874.
620 Wilson, C., Bolton, R., Busey, R., Lathrop, E., Dann, J., and Charsley-Groffman, L. 2019: End-of-Winter Snow Depth,
621 Temperature, Density and SWE Measurements at Teller Road Site, Seward Peninsula, Alaska, 2016-2018 [Data set],
622 doi: https://doi.org/10.5440/1592103.
623 Wilson, C., Dann, J., Bolton, R., Charsley-Groffman, L., Jafarov, E., Musa, D., and Wullschleger, S. 2021: In Situ
624 Soil Moisture and Thaw Depth Measurements Coincident with Airborne SAR Data Collections, Barrow and Seward
625 Peninsulas, Alaska, 2017 [Data set], doi: https://doi.org/10.5440/1423892.
626 Wrona, F. J., Johansson, M., Culp, J. M., Jenkins, A., Mård, J., Myers-Smith, I. H., … Wookey, P. A. 2016: Transitions
627 in Arctic ecosystems: Ecological implications of a changing hydrological regime. Journal of Geophysical Research:
628 Biogeosciences, 121: 650–674, doi: https://doi.org/10.1002/2015JG003133.
629 Yang, D., Meng, R., Morrison, B. D., McMahon, A., Hantson, W., Hayes, D. J., … Serbin, S. P. 2020: A Multi-Sensor
630 Unoccupied Aerial System Improves Characterization of Vegetation Composition and Canopy Properties in the Arctic
631 Tundra. Remote Sensing, 12: 2638, doi: https://doi.org/10.3390/rs12162638.
632

https://doi.org/10.5194/egusphere-2022-137
Preprint. Discussion started: 13 May 2022

633 **9. Figures**

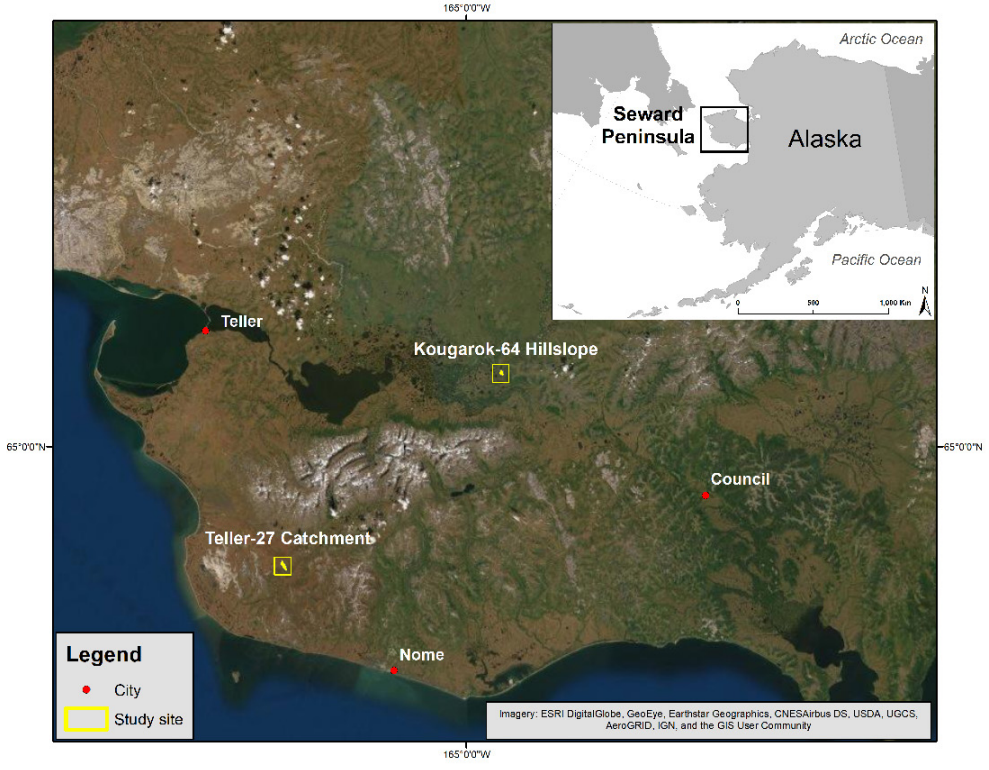

634

635 **Figure 1. Location of the Teller and Kougarok field sites with respect to the municipalities of Teller, Nome, and Council.**
636 **All are located on the Seward Peninsula in northwestern Alaska.**

637

https://doi.org/10.5194/egusphere-2022-137
Preprint. Discussion started: 13 May 2022

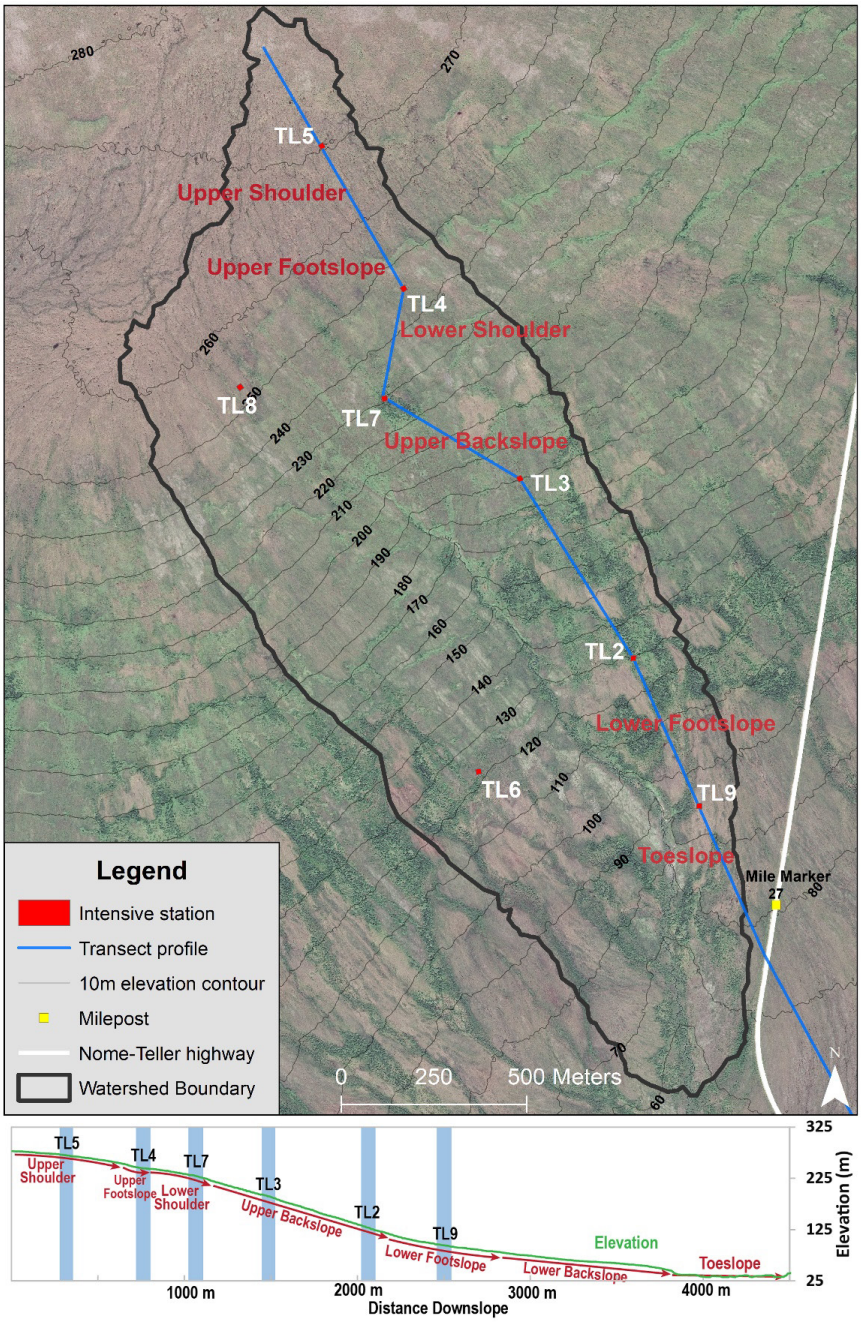

Figure 2. Topographic map of Teller. Station areas are shown as red polygons and the topographic station transect is given as a solid blue line. The hillslope transect elevation profile is given below the map in green, with stations along the transect in blue and hillslope positions noted with red arrows and text. RGB composite imagery from the 8-band WorldView-2 imagery obtained on July 27, 2011 at 1.5 m resolution downloaded from the DigitalGlobe website (https://www.digitalglobe.com/).

https://doi.org/10.5194/egusphere-2022-137
Preprint. Discussion started: 13 May 2022

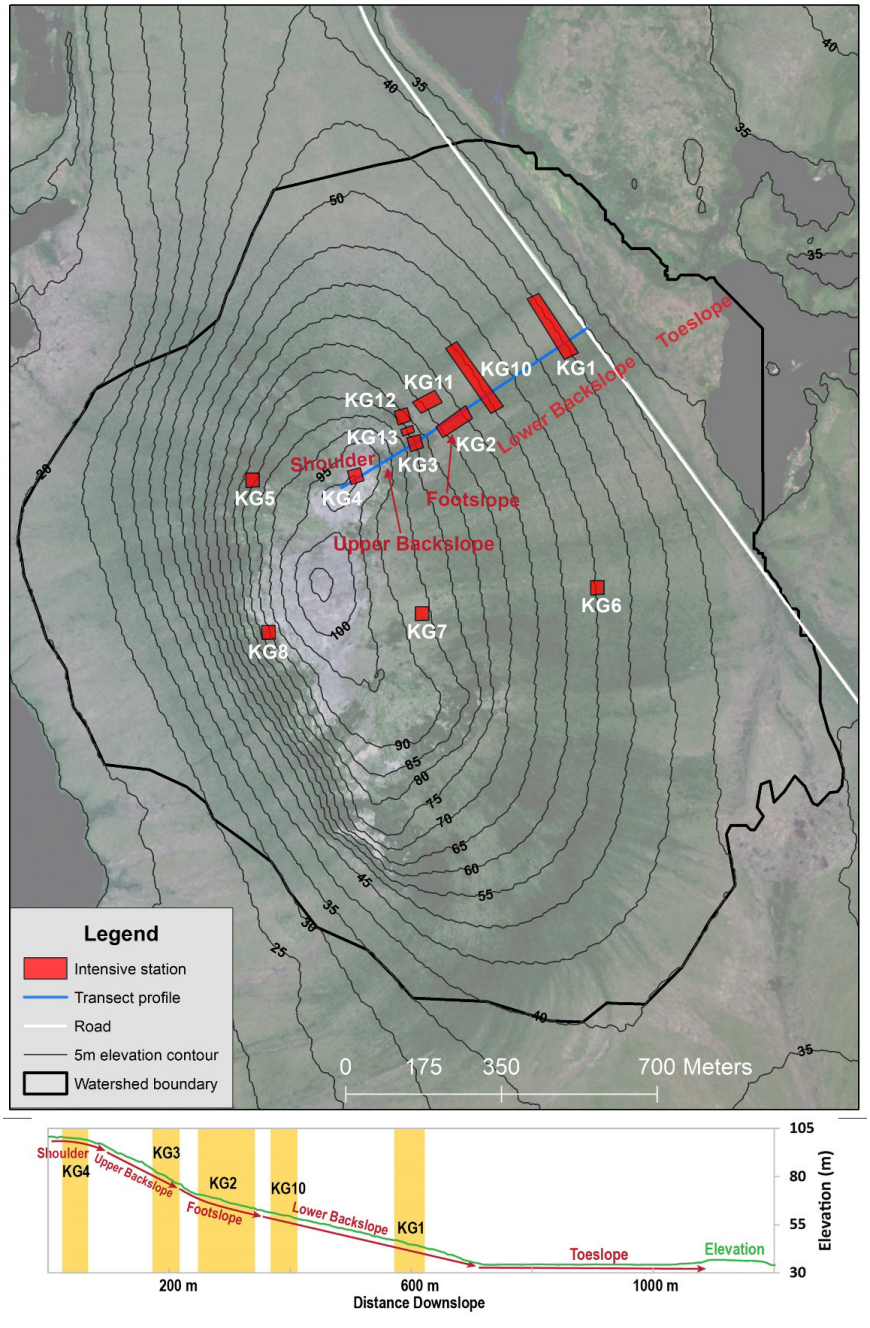

Figure 3. Topographic map of Kougarok. Station areas are shown as red polygons and the station transect is given as a solid blue line. The transect elevation profile is given below the map in green, with stations along the transect in yellow and hillslope positions noted with red arrows and text. RGB composite imagery from the 8-band WorldView-2 imagery obtained on July 14, 2017 at 1.5 m resolution downloaded from the DigitalGlobe website (https://www.digitalglobe.com/).

https://doi.org/10.5194/egusphere-2022-137
Preprint. Discussion started: 13 May 2022

650

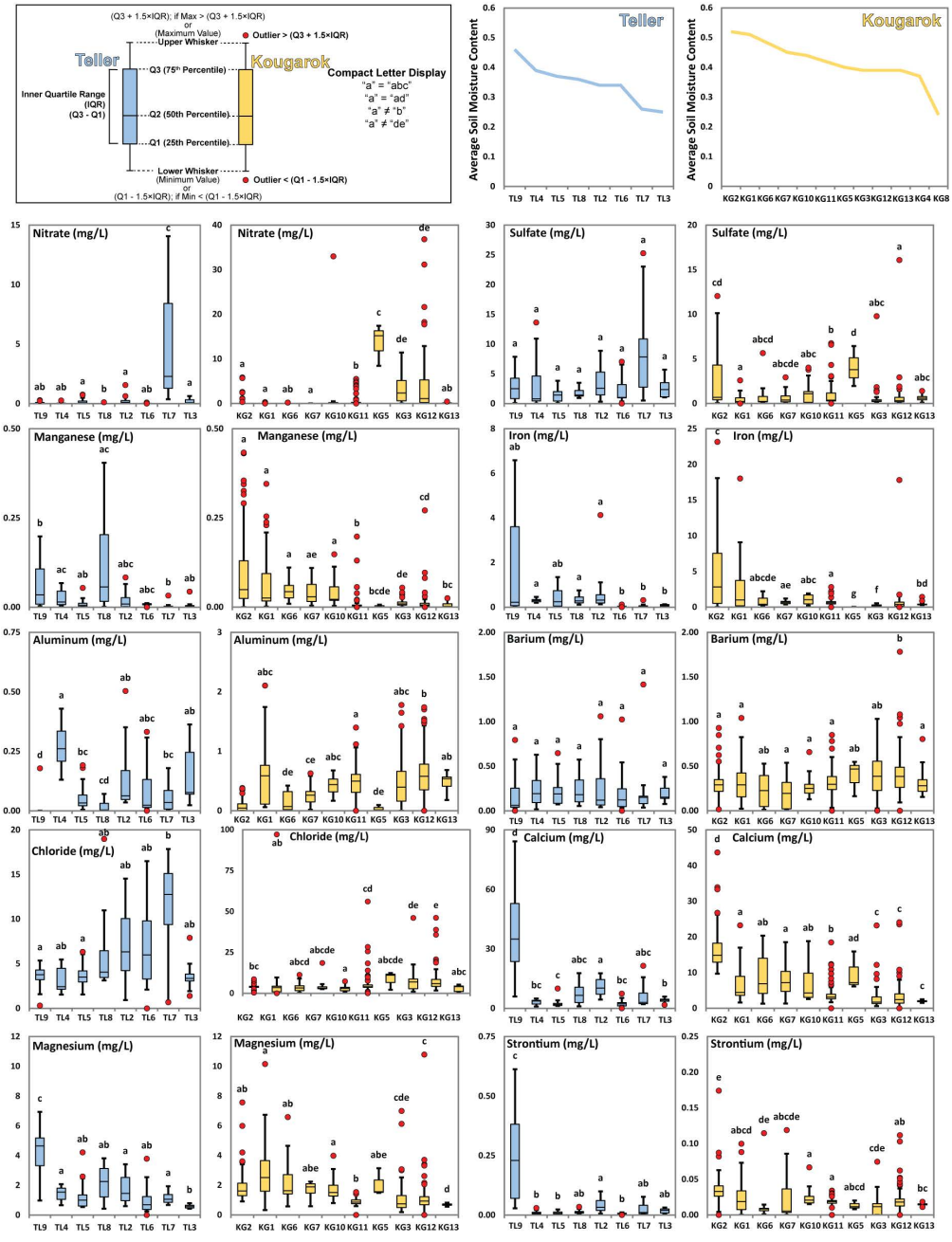

651

652 **Figure 4. Mean COI concentrations at Teller (blue) and Kougarok (yellow) stations. Stations are arranged (left to right) by**
653 **soil moisture content determined by P-Band SAR (top right). Boxplots show the first, second, and third data quartiles, with**
654 **box whiskers representing either 150% of the inner quartile range (IQR), or the maximum or minimum value, when that**
655 **value was less than 1.5×IQR. Red circles represent data points outside of the 1.5×IQR whiskers (i.e. outliers). Note that the**
656 **concentration scales on the Teller and Kougarok plots often differ.**

https://doi.org/10.5194/egusphere-2022-137
Preprint. Discussion started: 13 May 2022

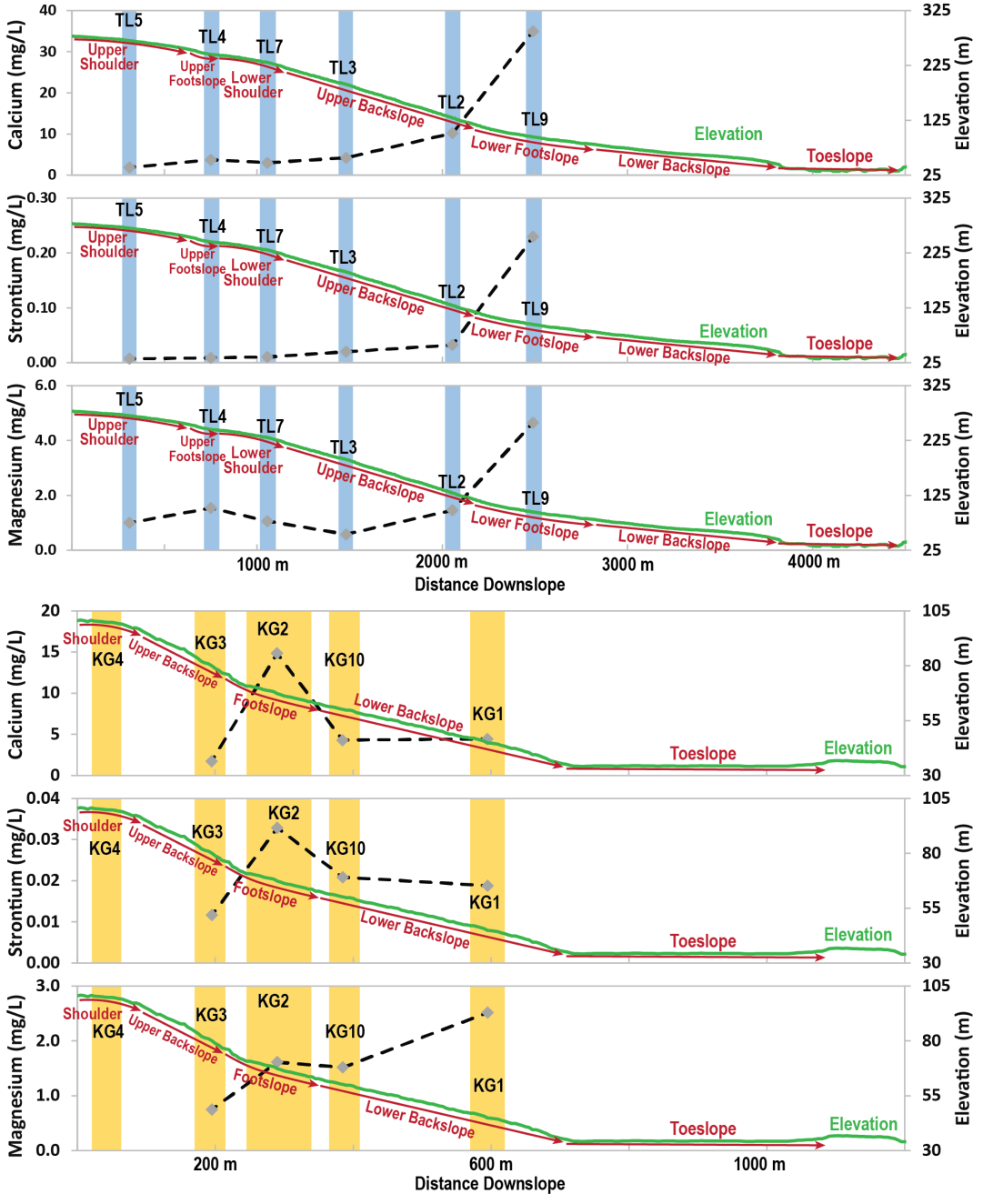

Figure 5. Median (50th percentile) concentrations (grey diamonds with dashed black lines) of Ca, Sr, and Mg, with distance downslope at Teller (blue) and Kougarok (yellow) along topographic transects; areas of stations are indicated by blue and yellow colouring, respectively. The elevation profiles of the hillslopes are plotted in green, on separate y-axes (right axes). Topographic regions of both catchments are indicated by red arrows along the elevation gradient.

https://doi.org/10.5194/egusphere-2022-137
Preprint. Discussion started: 13 May 2022

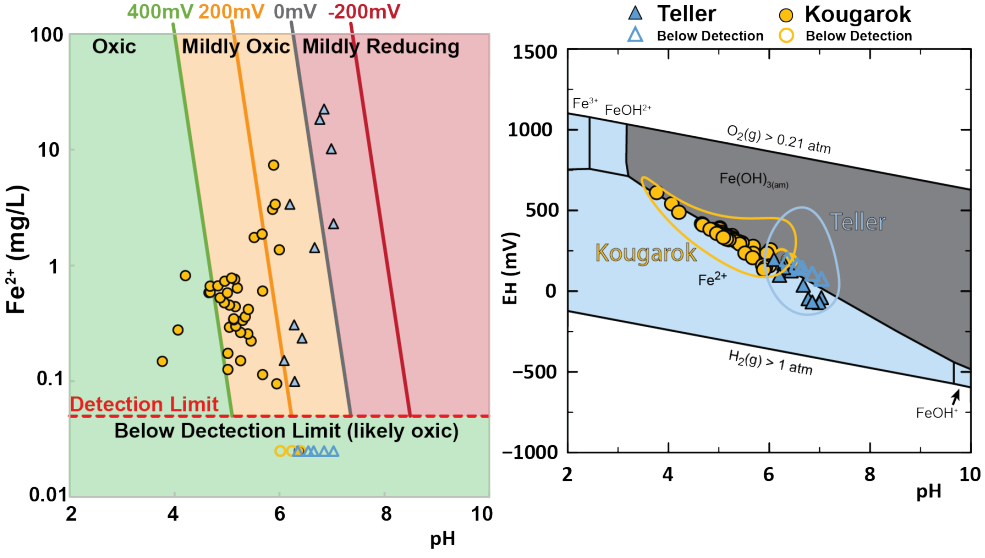

Figure 6. Left: Model-predicted Fe^{2+} concentrations in saturated solutions of $Fe(OH)_{3(am)}$ at fixed E_H conditions of 400 mV (green), 200 mV (orange), 0 mV (grey), and -200 mV (red), compared with field concentrations of Fe^{2+} at Teller (red circles) and Kougarok (yellow circles). Right: Fe predominance diagram, showing the dominant specie of Fe under a range of E_H/pH conditions. E_H/pH regions relevant to Teller and Kougarok are outlined in blue and yellow, respectively. Samples with Fe^{2+} concentrations below the detection limit are given as colour coordinated open circles set at 0.025 mg·L^{-1} (half the detection limit) in both sides of the figure.

https://doi.org/10.5194/egusphere-2022-137
Preprint. Discussion started: 13 May 2022

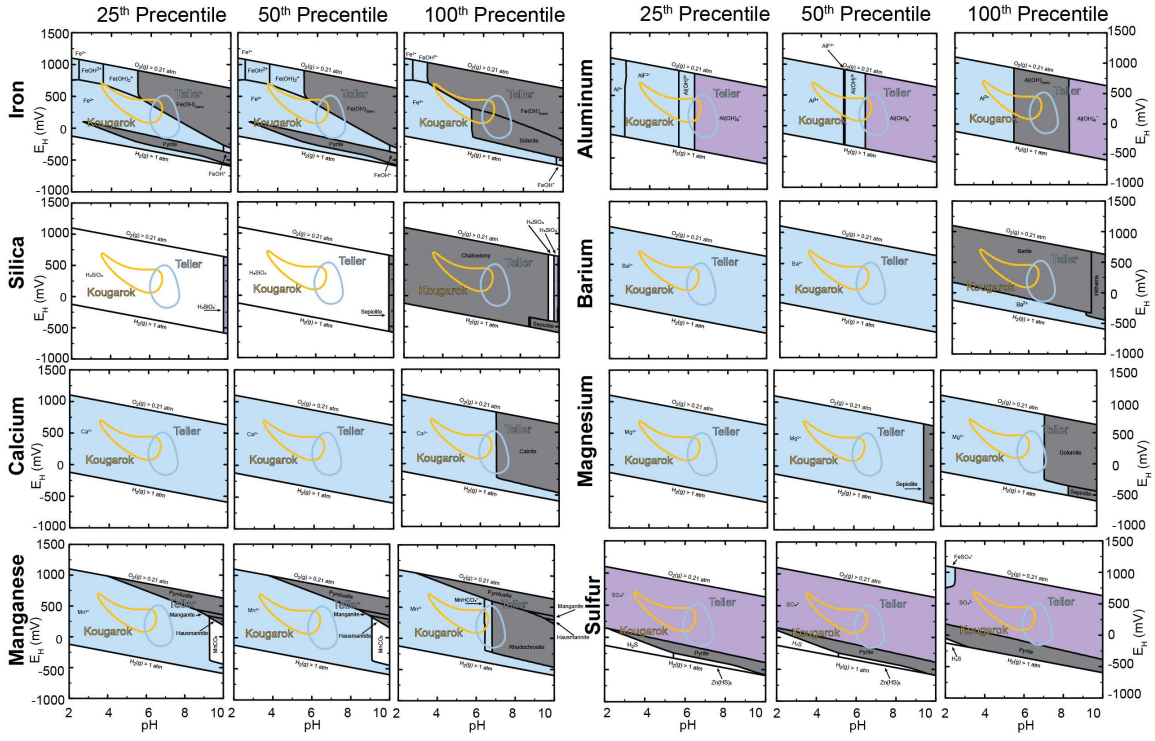

672

673 **Figure 7. E_H/pH diagrams for key species that indicated possible mineral formation under the E_H/pH conditions present at**
674 **either Teller or Kougarok. The E_H and pH conditions observed at Teller and Kougarok are overlaid as blue and yellow**
675 **lines, respectively. Mineral species (solids) are shown in grey, cations on are shown in blue, anions are shown in purple,**
676 **neutral species are shown in white. Predominance diagrams were created in PhreePlot using the phreeqc.dat database, with**
677 **inorganic carbonate reduction to methane "turned off."**

https://doi.org/10.5194/egusphere-2022-137
Preprint. Discussion started: 13 May 2022

678

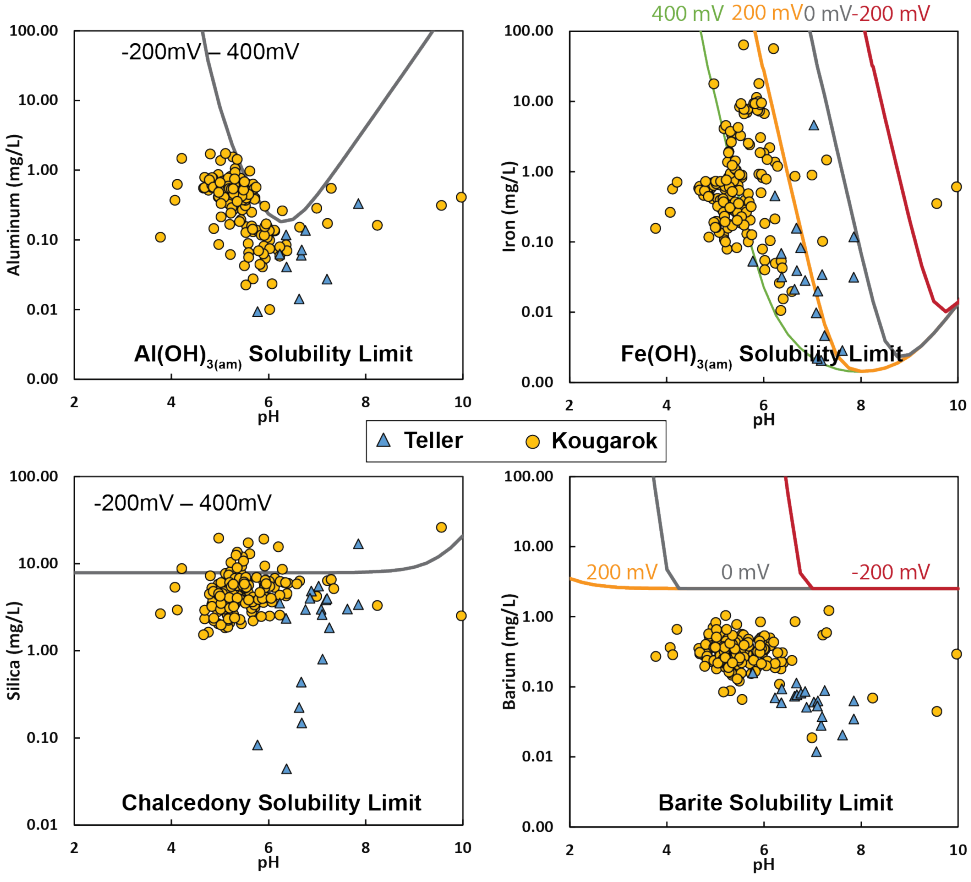

679

680 **Figure 8. Modelled solute concentrations in solutions saturated with $Al(OH)_{3(am)}$, $Fe(OH)_{3(am)}$, chalcedony, and barite, with**
681 **respect to pH (x-axis) and E_H (model lines), overlaid with observed solute concentrations.**

682

https://doi.org/10.5194/egusphere-2022-137
Preprint. Discussion started: 13 May 2022

10. Tables

Table 1. Teller Station Physical Characteristics

		Vegetation				*Relative wetness*			*Permafrost*		
	Hillslope Position	Vegetation type	Average (maximum) canopy height (cm)	Dominant PFT	Low to tall shrub cover	Average TDR soil moisture (VMC)	Average P-band SAR (VMC)	Average snow depth (cm)	Average Ground Temperature (°C)	Permafrost Extent	Average (maximum) thaw depth (cm)
TL9	Lower Footslope	Wetland complex	34 (41)	Graminoid	10	NA	0.46	68.4	0	Marginal	101 (>120)
TL5	Upper Shoulder		31 (45)		7	0.55	0.37	103.3	-0.45	Near-surface	97[r] (>114[r])
TL8	Upper Footslope		17 (34)		20	0.55	0.36	77.7	-0.6		69[r] (>120)
TL3	Upper Backslope	Cassiope dwarf shrub tundra	13 (23)	Evergreen dwarf shrub	4	NA	0.25	62.1	2.2	None/ deep	72[r] (82[r])
TL4	Upper Footslope		10 (14)		12	0.35	0.39	89.5	0.5	Marginal	40[r] (70[r])
TL2	Upper Backslope	Mesic willow shrubland	132 (141)	Deciduous low to tall shrub (willow)	44	0.4	0.34	124	2.4	None/ deep	75[r] (>120)
TL7	Lower Shoulder		168 (189)		37	0.46	0.26	128.8	2.4		51[r] (66[r])
TL6	Upper Backslope	Willow-birch tundra	74 (115)	Deciduous low shrub (willow & birch)	32	0.38	0.34	86.4	1.2	None/ deep	67r[r] (102[r])

PFT – plant functional type; dwarf shrub (height <40 cm), low shrub (height 40-200 cm), low to tall shrub (height 40 to >200 cm tall).
[1]Single point soil moisture measurements. Data are more accurate than P-band SAR but represent a much smaller spatial scale.
[2]P-band SAR has 30m resolution.
[r] Resistive layer was rock; all others are permafrost. A temperature probe was used to determine if the resistive layer was permafrost (≤0 °C) or rock (>2 °C). Thaw depth is an average of 4 measurements from the vegetation plot corners within the IS and was measured at the end of the growing season.

https://doi.org/10.5194/egusphere-2022-137
Preprint. Discussion started: 13 May 2022

693 **Table 2. Kougarok Station Physical Characteristics**

		Vegetation				*Relative wetness*			*Permafrost*		
	Hillslope Position	Vegetation type	Average (maximum) canopy height (cm)	Dominant PFT	Low to tall shrub cover	Average TDR soil moisture (VMC)	Average P-band SAR (VMC)	Average snow depth (cm)	Average Ground Temperature (°C)	Permafrost Extent	Average (maximum) thaw depth (cm)
KG3	Upper Backslope	Alder shrubland	204 (265)	Deciduous low to tall shrub (alder)	30	0.19	0.39	131.3	-0.01	Near-surface	48[r] (53r)
KG12	Footslope		NA		NA	0.30*	0.39	NA	NA		NA
KG1	Lower Backslope	Alder savanna in tussock tundra	60 (90)	Deciduous low shrub (alder, willow & birch)	13	NA	0.51	83.4	-2.5	Near-surface	61 (68)
KG2	Footslope		48 (73)		20	0.63	0.52	102.3	-1.2		75 (89)
KG6	Lower Backslope		24 (61)		0	0.36	0.48	66.2	-2.2		58 (62)
KG10	Lower Backslope		NA		NA	NA*	0.44	71.4	NA		NA
KG11	Footslope		NA		NA	0.59*	0.42	NA	NA		NA
KG7	Upper Backslope	Tussock-lichen tundra	20 (22)	Graminoid	0	0.51	0.45	54.7	-2.1	Near-surface	76 (100)
KG4	Shoulder	Dryas-lichen shrub tundra	6 (12)	Evergreen dwarf shrub	0	NA	0.37	NA	-1.9	Near-surface	0[r] (0[r])
KG13	Upper Backslope		NA		NA	0.41*	0.39	92.1	NA		NA
KG5	Upper Backslope	Willow-birch tundra	62 (137)	Deciduous low shrub (willow & birch)	3	NA	0.4	178.4	> 0	Deep	88 (96)
KG8	Upper Backslope		45 (120)		42	0.23	0.24	85.5	-0.04	Near-surface	44[r] (55[r])

694
695 Note: PFT – plant functional type.
696 [1]Single point soil moisture measurements. Data are more accurate than P-band SAR but represent a much smaller spatial scale.
697 [2]P-band SAR has 30m resolution.
698 *Average gravimetric water content measurements, corrected to VMC by bulk density.
699 [r]Resistive layer was rock; all others are permafrost. A temperature probe was used to determine if the resistive layer was permafrost (≤0 °C)
700 or rock (>2 °C). Thaw depth is an average of 4 measurements from the vegetation plot corners within the IS and was measured at the end of
701 the growing season.

https://doi.org/10.5194/egusphere-2022-137
Preprint. Discussion started: 13 May 2022

Table 3. Inter-Site Mann-Whitney U-Test Results

	Teller			Kougarok						
	n	$\sum R_i$	U_i	n	$\sum R_i$	U_i	|z|	Site with Higher Median	Effect Size	Difference in Correlation
Na	59	3184	14811.5	275	52761.5	1413.5	**9.95**	Kougarok	0.54	large
F	59	3502	14375.5	273	51776.5	1731.5	**9.46**	Kougarok	0.52	large
K	59	3882	14113	275	52063	2112	**8.92**	Kougarok	0.49	medium-large
Si	59	4119	13876.5	275	51826.5	2348.5	**8.56**	Kougarok	0.47	medium-large
Al	58	4952	12709	275	50659	3241	**7.11**	Kougarok	0.39	medium
Oxalate	57	4996	12161.5	272	49289.5	3342.5	**6.75**	Kougarok	0.37	medium
B	59	5429	12566.5	275	50516.5	3658.5	**6.62**	Kougarok	0.36	medium
Zn	58	5605	12056	275	50006	3894	**6.12**	Kougarok	0.34	medium
SO_4	58	13653	3892.5	273	41293.5	11941.5	**6.08**	Teller	0.33	medium
Fe	58	5958	11703	275	49653	4247	**5.60**	Kougarok	0.31	medium
Ba	58	6256	11405.5	275	49355.5	4544.5	**5.15**	Kougarok	0.28	medium
Ti	58	6266	11395.5	275	49345.5	4554.5	**5.13**	Kougarok	0.28	medium
NO_2	54	5588	10585.5	272	47713.5	4102.5	**5.12**	Kougarok	0.28	medium
Li	58	7778	9883	275	47833	6067	**2.86**	Kougarok	0.16	small-medium
Br	58	8485	9060.5	273	46461.5	6773.5	1.73	Equal	0.09	small
NO_3	58	8576	8969	273	46370	6865	1.59	Kougarok	0.09	small
Sr	58	8683	8978	275	46928	6972	1.51	Kougarok	0.08	small
PO4	54	9659	6460.5	271	43316.5	8173.5	1.36	Equal	0.08	small
Mg	58	10495	7166	275	45116	8784	1.21	Teller	0.07	small
Cr	58	8884	8777	275	46727	7173	1.20	Kougarok	0.07	small
Mn	58	9164	8497	275	46447	7453	0.78	Teller	0.04	small
Cl	58	9221	8266.5	272	45394.5	7509.5	0.57	Kougarok	0.03	small
Ca	58	10016	7645	275	45595	8305	0.50	Teller	0.03	small

Table 4. Dominant Environmental Controls on SPW Geochemistry at Teller and Kougarok

Environmental Control	Analytes Affected
Vegetation	NO_3
Soil Moisture/Redox	NO_3, Mn, Fe, SO_4 (occasionally)
Water/Soil Interactions & Hydrologic Transport	Ca, Mg, Sr
Mineral Solubility	Al, Ba, Si, Fe